

EFFECT OF BLADE SHAPE ON THE CHARACTERISTIC OF UNSHROUDED CENTRIFUGAL PUMP

Nur Kaliwantoro*) and Sutrisno

Departement of Mechanical and Industrial Engineering, Gadjah Mada University,
Jl. Grafika 2 Yogyakarta. 52281
E-mail: sutrisno@ugm.ac.id

*) Teaching staff member of the Department of Mechanical Engineering, University of Mataram

Abstract

Effect of blade shape on the flow patterns, performance and pressure distributions along the shroud of centrifugal pump has been studied. Five unshrouded impellers having different inlet and outlet angle: 30° - 20° , 30° - 30° , 30° - 40° , 30° - 50° and 40° - 40° , each, were employed six flow capacities. Flow patterns on the impeller were investigated using wet paint while the pressure distributions were measured using simple pitot tubes that was mounted on the shroud surface.

It is found that among the impellers having the same inlet angle of 30° , impeller with configuration of 30° - 40° has the best efficiency 50.04% when employed at condition of 273 lpm and the ratio of tip clearance to blade height of 1.89/17, while impeller with configuration 30° - 50° has the highest of pressure coefficient, 0.393, when employed at the same condition. In the visualization, there are traces of horseshoe vortex around the blade. This vortex separates its self into the pressure side leg of the horseshoe vortex and the suction side leg of the horseshoe vortex. Along the blade this suction side vortex increases its dimension and becomes the passage vortex which at last interferes the path of mainflow. Whereas the measurement of pressure distribution shows that the static, radial and tangential pressures increase as the distance of measurement from the center of the shroud is increased. It is also investigated that impeller with long passage causes lower tangential, meridional and static pressures along the shroud than those of the impeller with shorter passage. Although the pressures is lower, but the value of (PT-Ps) and (Pm-Ps) of long passage impeller are greater than those parameters of the impeller with short passage. Indirectly, it indicates that the leakage capacity of long passage impeller is greater than that of shorter passage impeller.

Keywords: unshrouded impeller, blade shape, pressure distributions, flow visualization

INTRODUCTION

Centrifugal pump is a type of pump that has been well known and widely used in daily life. A lot of centrifugal pumps have been produced in this country, even some small industries have been able to produce several kinds of them. Generally, the marketing of pumps produced by local industries are only inside of this country with limited market penetration. This condition happens besides due to the lack of good marketing management, also caused by the local products which are not competitive in performance and design if compared to the similar products produced by large industries or imported pumps.

Pump performance is mainly affected by two factors, namely the impeller design and pump casing. Many factors affecting the design of high performance impeller, some of them are the passage length and impeller inlet and outlet angle. The above factors affect each others and usually optimizing depends on final purpose of the pump.

Dimensions and dynamic motion of pump elements, especially which are contacting within the fluid, affect the flow patterns and at last determine the pump performance. Although many experimental and computational studies in centrifugal pump had been performed in the past, detail description especially which respect to the flow patterns developed inside of the pump due to variation of impeller geometry have not been completely explored yet. Based on this fact, more detail experimental work on the flow patterns in impeller for various blade shapes is required in order to get better design for promoting the local product pump. For getting a more comprehensive study, distribution of tangential and radial as well as static pressures on the shroud surface were also investigated.

Murakami, Kikuyama and Asakura (1980) observed velocity and pressure distributions, and flow pattern in the impeller passages of centrifugal pump with three and seven blades, respectively. Velocity and pressure distributions were measured using yaw probe that are attached on hub, while visualization method using oil surface was adopted to observe flow pattern inside the impeller. It was obtained that velocity and pressure distribution at impeller passages having seven blades shows congruity with the theoretical calculation. While impeller having three blades yielded velocity and pressure distribution which deviate from the theoretical calculation. This deviation was occurred due to appearance of secondary flow with high intensity, which easily to appear in wider passage space of the three blades impeller.

Suryoprato (1999) simulated effect of curvature, thickness and numbers of blades on the performance and flow pattern of the NS-50 type unshrouded centrifugal pump. CFD-Fluent was employed for developing this two dimensional simulation. This research resulted that the best impeller, which having smallest separation in its passages, belongs to impeller with seven blades, 4 mm blades thickness and inlet and outlet angle of 41.4° and 32.9°, respectively.

Hah and Krain (1990) a part of their study is to investigate the pressure distribution along the shroud of a compressor having high-efficiency backswept impeller with 30° outlet angle. They obtained that the pressure distributions were affected by the condition of flow capacity. At the choke condition there was pressure drop at the leading edge especially at $x/s_m = 0.1$. Such phenomenon could not be found at surge condition. When the condition was setted to design condition, the pressure distribution obtained was almost similar as found at surge condition.

Fluid flows in turbomachinery are always three-dimensional, viscous and unsteady. In case of centrifugal machines, there are strong viscous effect and significant region of flow with separation and secondary flow. The flow field is very complex, three-dimensional and turbulent all under the influence of curvature and rotation (Lakshminarayana, 1996).

The centrifugal machine achieves part of the pressure rise from the centrifugal and Coriolis forces due to rotation and the change of radii. This is in addition to the pressure rise achieved through the flow-turning as in axial ones, where the interchange is through the change of tangential momentum. In view of the large pressure rise and the presence of centrifugal and Coriolis force fields, the flow through the centrifugal passages is affected adversely by the large boundary layer growth, flow separation and secondary flow.

Secondary flow is defined as the deviation of primary flow from the primary flow direction. This flow can be developed due to the existence of the gradient in stagnation pressure in the passage, and in many instances this flow rolls up into vortices. This flow also introduces cross flow (v and w) velocity component, which results in three-dimensionality in the flow field. The secondary flow losses include some of the kinetic energy in secondary velocities as well as losses associated with the formation, development, diffusion and dissipation of these vortices. In many cases secondary flow is also responsible cavitation and resulting deterioration in performance and damage in liquid handling machinery.

Deviation on the mainflow due to the secondary flow is affected by angle of divergence of the impeller as indicated by :

$$\left(\frac{\partial p}{\partial n}\right)_A = \frac{\rho u_A^2}{R_A} \quad (1-1)$$

$$\left(\frac{\partial p}{\partial n}\right)_A = \left(\frac{\partial p}{\partial n}\right)_B = \frac{\rho u_A^2}{R_A} > \frac{\rho u_B^2}{R_B} \quad (1-2)$$

where P represent pressure, R is radius and u is the total streamwise velocity. While A and B represent the respective suction side and pressure side.

The superimpose of the complex flows which occurs in the passage causes the formation of many kinds of vortex, includes leakage flow vortex, secondary vortex and

corner vortex or horseshoe vortex. Commonly, the horseshoe vortex is divided into two types, suction side leg horseshoe vortex and pressure side leg horseshoe vortex.

PROCEDURE OF THE RESEARCH

A. Testing Material

This research employed five unshrouded centrifugal impellers, each with different vane curvature, as testing materials. Those impellers were designed using arcus tangent method according to below equation:

$$\rho = \frac{R_b^2 - R_a^2}{2(R_b \cos \beta_b - R_a \cos \beta_a)} \quad (1-3)$$

Here symbol a and b represents inlet and outlet, respectively. Each vane curvature had two arcs which coincide at the point having comparison 4:1, measured accordingly to the meridional length of impeller.

Inlet angle was fixed to value 30°, which was taken to compromise the difference of the inlet angle between the original impeller that had value 41,4° to those as suggested in the text book that had range from 15° up to 35°. While the value of outlet angle were 20°, 30°, 40° and 50°. Original impeller having inlet and outlet angle of 41,4° and 41,4°, each, were also made as reference

Table 3-1. Data of testing impeler

	Impeller 1	Impeller 2	Impeller 3	Impeller 4	orginal impeler
Inner diamater (mm)	46	46	46	46	46
Outer diameter (mm)	165	165	165	165	165
Blade height (mm)	17	17	17	17	17
Blade thickness (mm)	5	5	5	5	5
Inlet angle (°)	30	30	30	30	41,4
Outlet angle (°)	20	30	40	50	41,4
Blade length (mm)	116,99	101,42	85,29	82,66	88,19
Passage wide (mm ²)	2701,81	2779,66	2860,31	2873,47	2845,83

For complying the request of better accuracy, those testing material were made using CNC machine which belonged to CNC Laboratory of Mechanical Engineering of Gadjah Mada University. The requirement of Alumunium blocks was supplied by PT. Baja Apik, Cepur, Klaten.

B. Equipment

- a. Pump NS-50 with unshrouded centrifugal impeller
- b. Piping installation using PVC pipe with 2 inch diameter
- c. Three phase electric motor, 2 hp equipped by a wattmeter
- d. Flowmeter, stroboscope, manometer, pitot tube and camera

C. Procedure

1. Performance Testing

1. The tip clearance height was measured
2. After the motor was turned on, flow capacity was setted to its smallest flow capacity.
3. After the flow reached its steady condition, measure the suction and discharge pressure, pressure gradient of the orifice, rotation of the impeller, voltage and current of the electric motor.
4. Step 3 was repeated for another flow capacities
5. Step 4 was repeated for another impellers having different vane curvature
6. Step 5 was repeated for another tip clearance heights.

2. Flow Visualization

- a. Disassemble the impeller and clean it. Spray red paint over the impeller surface. This spraying was done in such away that the paint layer was looked like to be the same in thickness. After exposed to open air, this impeller was sprayed again using yellow paint. Through the similar procedure, white paint and blue paint were sprayed over the impeller surface,
- b. This impeller which has been covered with four paint layers was assambled again into the the pump casing using the same tip clearance height as applied in performance testing,
- c. Turns the electric motor on and sets the pump capacity to 250 lpm. For complying the guarantee in which the pump rotates and flows fluid in its steady condition, the pump was turned on for 30 seconds,
- d. The impeller was disassambled again and the flow pattern on impeller surface that was formed due to exposing to fluid flow, was photographed, For convenient, the photograph was taken for at least twice.
- e. Reclean this impeller for reuse,
- f. Steps a to f was repeated for another impeller with different vane curvature,

3. Measurement of Pressure Distributions Along the Shroud

Measurement was performed for investigating static, tangential and radial pressure distributions along the shroud. Since the type of employed impellers come from the unshrouded type, hence the term shroud here is refer to the shroud of pump casing.

Each impellers in this testing were exposed to four flow conditions, viz: 95 lpm, 195 lpm, 250 lpm and 306 lpm. The measurement was done using simple probe having four measurement points which were made of copper pipes with 1.5 mm inner diameter. This measurement points were located in radial direction of 25, 43.5, 60 and 74.5 mm from the shroud center with angle of 225° from the tongue. As measurement that was performed in earlier stages, the procedure in this stage was also very similar to those as told in performance testing. The additional step was the measurement of those static, tangential and radial pressure inside the pump casing.

RESULT AND DISCUSSION

A. Interpretation of Flow Based on Paint Trace on Impeller Surface

In this study, effort of simplified interpretation of flow is devided into four sections. Those are the flow pattern on hub surface, wall of pressure side, wall of suction side and tip surface. Flow pattern on hub yielded by impeller having inlet and outlet angle 30° and 50° , respectively, employed under 1800 rpm is shown in figure 3-1.

As seen in the figure, at the leading edge of the vane, the horseshoe vortex separates itself into the suction side leg of the horseshoe vortex and the pressure side leg of the horseshoe vortex. At first these horseshoe vortexs are small enough and they do not interfere the path of the mainstream. But as the area becomes wider, at r/r_o about $1/3$, these vortexs, especially the suction side becomes larger and begins to interfere and causes the deviation to the flowpath from its ideal path. At last the suction side of the horseshoe vortex dominates the passage and becomes the passage vortex.



©

Figure 3-2. Flow pattern on the wall of pressure side (a), on the wall of suction side (b) and their interpretation (c)

Such deviation to the mainflow is clearly seen by the appearance of the yellow paint on the hub surface. On the corner of pressure side the yellow color with lower intensity is appeared. It indicates that in such condition, the intensity of the suction side leg of the horseshoe vortex is larger than the pressure side leg of the horseshoe vortex.

B. Effect of Blade Curvature

Effect of blade curvature on the flow pattern of impellers having combination of β_1 and β_2 of 30°-20°, 30°-30°, 30°-40° and 30°-50°, each, employed under the same condition where ratio of c/b is 5.6/17 and flow capacity is 273 lpm, are shown in figure 3-3.

Impeller having short vane will has large angle of divergence and wider passage area. This condition is bad since fluid can not be directed into its ideal path when it pass through the passage due to the existence of vortex generation as explained earlier. The wider space also gives the possibility to the fluid to be reversed and tends to flow back. At last the combination of the vortex generation and the reversed flow will interfere the fluid to flow with deviation from its ideal path. This phenomenon is clearly seen in figure 3-1 of the earlier section.

Differs with condition of impeller having combination of β_1 and β_2 of 30°-50° where its yellow color is concentrated on the suction side due to the existence of flow reversion and generation of suction side vortex, on the second impeller with of β_1 and β_2 of 30°-20°, its yellow color spreads on the larger area compared to the first impeller.

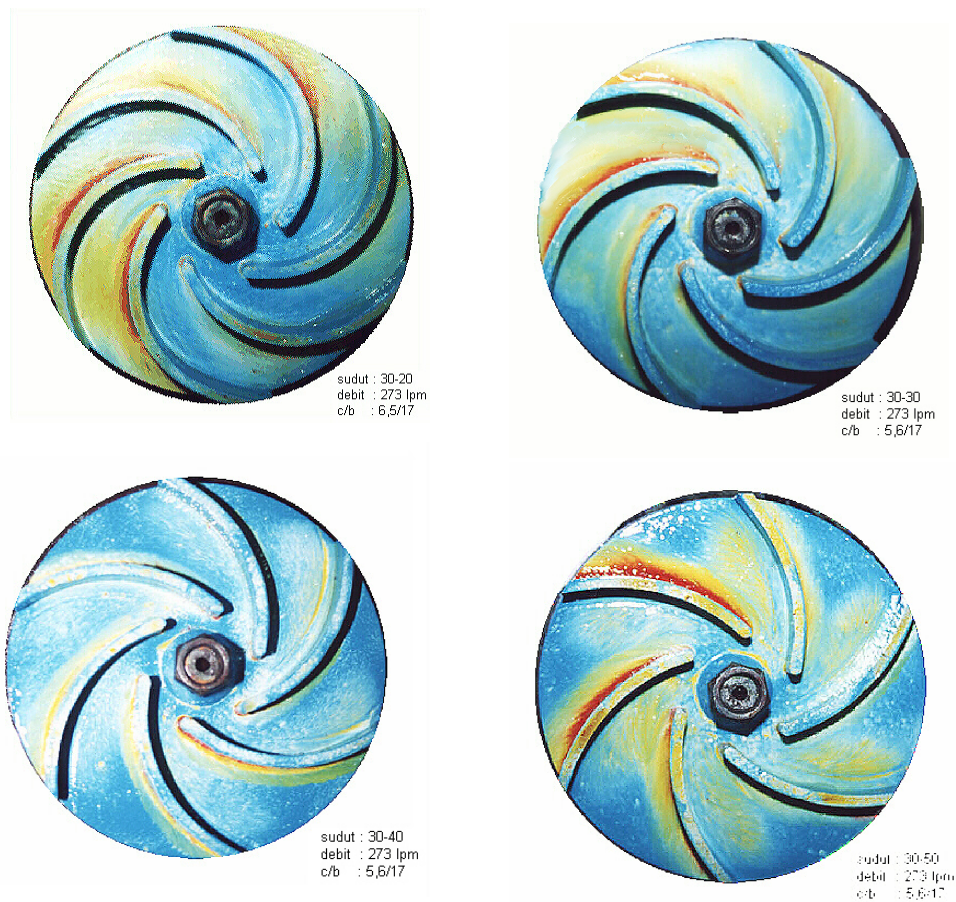


Figure 3-3. Effect of blade curvature on flow pattern



Figure 3-4. Flow pattern in impeller 30-40 (left) and impeller 30-20 (right)

When respected to the geometrical shape where its β_1 and β_2 are 30° and 20° , this larger spread of yellow color is likely to be happened due to the generation of larger pressure side leg of the horseshoe vortex. The pressure side vortex exists since the fluid can not maintain its path close to blade due to the blade shape which is too buckling. The dimension and intensity of this pressure side vortex are larger than the suction side vortex. Since the vortex tends to extend its shape as it goes downward, the both suction side and pressure side vortex combine their shape as they move near the outermost region. This condition is marked by the yellow color with high enough intensity in the outermost region as seen in figure 3-4 (right).

Fluid motion in impeller having β_1 and β_2 of 30° and 40° is likely to more follows its ideal path. Blue color dominates almost the whole passage, which indicates that fluid motion is almost undisturbed by vortex generation. This condition causes the ratio of real fluid velocity to the ideal fluid velocity becomes larger compared with another impellers. While a little yellow color in the suction side region is likely to be caused by wake of the fluid motion. This conclusion is based on fact that position of yellow color is placed on the collision region between the wall of suction side and the inlet fluid, where its direction is changed from axial to radial.

The flow pattern inside the channel highly controls the overall performance yielded by each impeller. Figure 3-5 shows the efficiency of each impeller, examined under several flow capacity. It is seen that when employed in the design capacity, $Q = 273$ lpm, impeller with combination of β_1 and β_2 are 30° and 20° , has the lowest efficiency, eventhough when compared with the impeller having β_1 and β_2 are 30° and 50° .

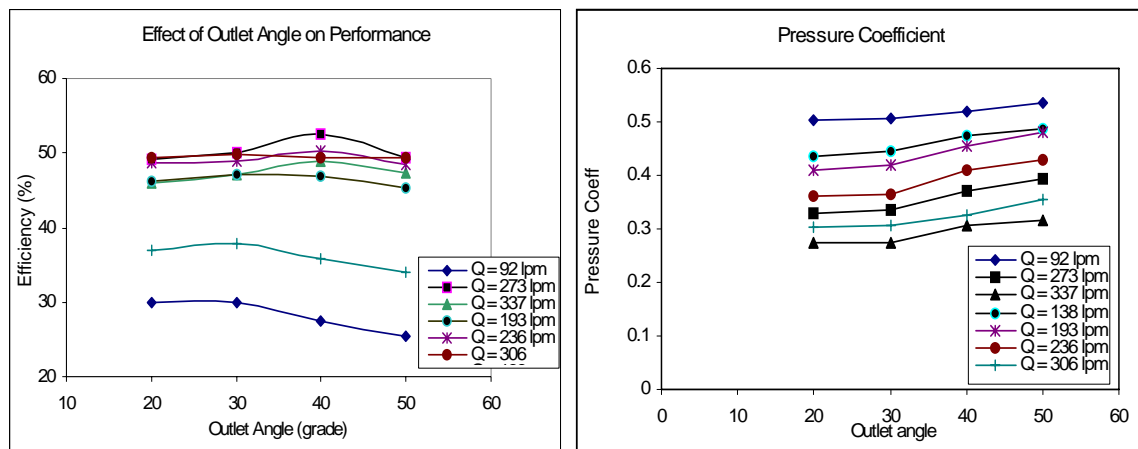


Figure 3-5. Effect of blade curvature on flow pattern

This result indicates that the effect of combination of the horseshoe vortex as well as friction loss in reducing the efficiency is more significant than the effect of flow deviation due to excessive angle of divergence. Among the tested impellers, the most efficient belongs to impeller with inlet and outlet angle 30° and 40° . When respected to the flow pattern as discussed earlier, this result is not so suprisingly since impeller with such combination has the best flow pattern among those impellers. As shown in figure 3-5 the result is also valid when the flow capacity is increased passed to its design capacity, which in this case is performed in capacity 337 lpm.

Deviation occurs when its capacity is decreased far below its normal capacity, where in this investigation the capacity is set to 92 lpm. The efficiency of impeller with configuration of 30° - 20° is higher than impeller of 30° - 50° , eventhough when compared with the impeller of 30° - 40° . When related to flow pattern as found in the next section, this phenomenon exists since the fluid in impeller 30° - 40° and 30° - 50° experiences greater secondary flow due to wider passage area which in turn decreased their efficiency. While in impeller 30° - 20° and 30° - 20° such phenomenon do not occur since their passage areas are relatively small. Deviation is also occurred at capacity 193 lpm.

2. Pressure distribution on the shroud

Pressures measured in this experiment are static pressure, tangential pressure and meridional pressure. With the help of aluminium sheet the pitot tube made of copper pipe with inner diameter 0.5 mm and 1.85 mm of outer diameter was mounted on the shroud surface. The pressures were measured on six nodes as seen in figure 4-6 and detail are listed on table 4-2.

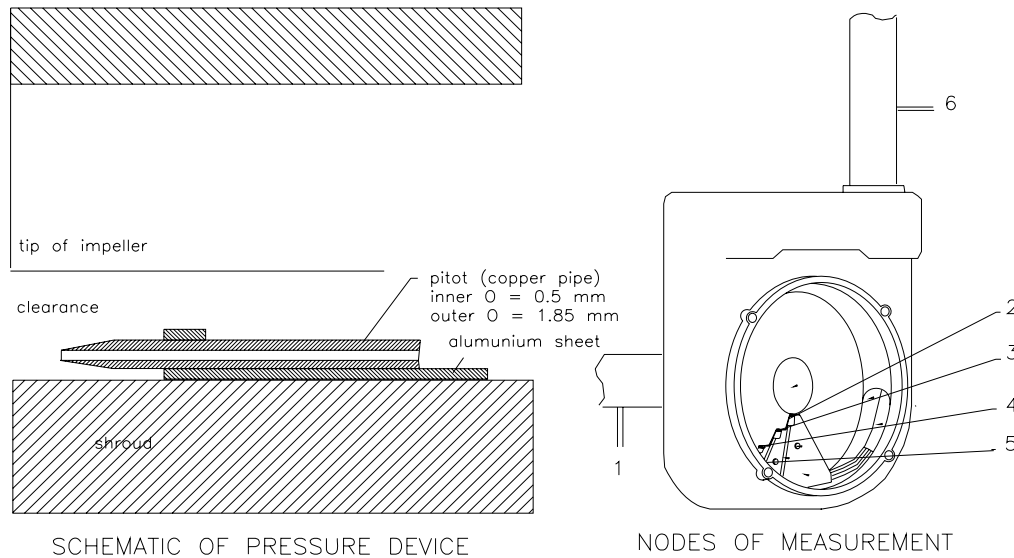


Figure 4-6. method of pressure measurement on the shroud surface

Table 4-2. Node of measurement

Node	1	2	3	4	5	6
Location from the center	suction	25 mm	43.5 mm	60 mm	74.5 mm	discharge

As presented by figure 4-7 (a), the pressure on the node close to the center of shroud is lower than the suction pressure which is measured 10 cm from the suction hole. As the distance is increased, the static pressure increases which indicates that energy converted to the head of the fluid increases. This pattern has a good accordance with the result of Krain where the test machine is a compressor with semi open impeller as given by figure 4-7 (b).

Almost similar patterns are also showed by the result of meridional and tangential pressure distributions as seen in figure 4-7. Both pressure distributions have the same behaviour, when the capacity is setted to a little one the pressures on the outermost of the shroud are lower than the discharge pressures. But when the capacity is increased to 250 lpm or 306 lpm, the pressures on the outermost of the shroud become larger than the discharge pressures.

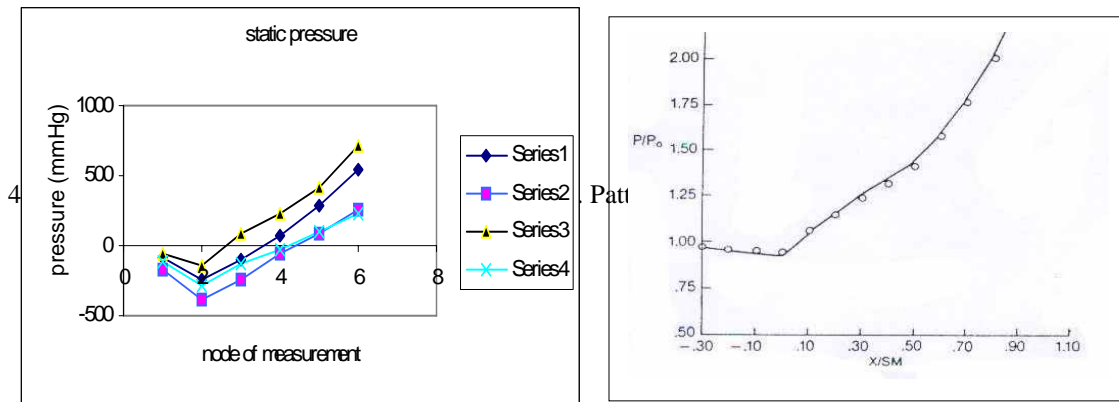
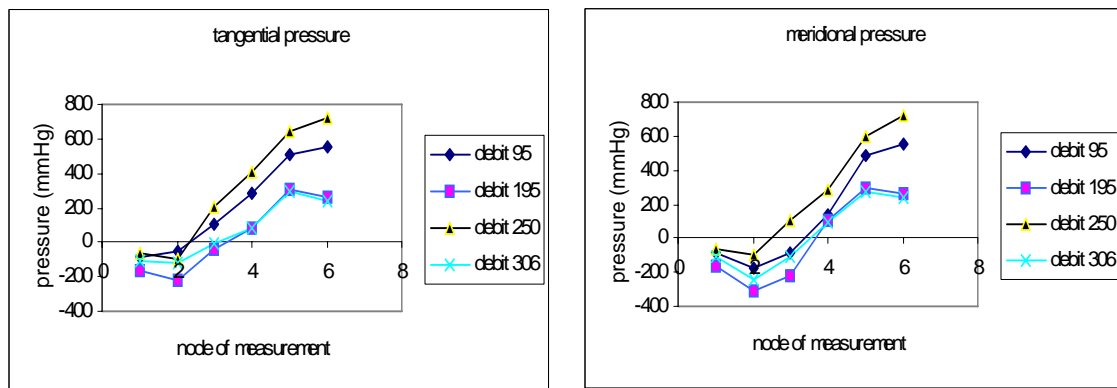


Figure 4-7c. Pressure distribution along the shroud with of impeller 30-40, $c/b = 6.2/17$

Effect of blade curvature on the characteristic of pressure along the shroud is given by figure 4-8. As mentioned earlier the performance of impeller 30° - 20° , includes head and efficiency, is lower than that of impeller 30° - 40° . In fact, the lower in head above is followed by the lower of pressure along the shroud, when compared to the impeller 30° - 40° .



Another thing that should be noticed in respect to the effect of blade curvature on the pressure along the shroud is the value of $(P_T - P_s)$ and $(P_m - P_s)$. Although the pressures of static, tangential and meridional of impeller 30° - 20° are lower than those of impeller 30° - 40° , but the values of $(P_T - P_s)$ and $(P_m - P_s)$ of impeller 30° - 20° are higher, almost double if compared with the similar values of impeller 30° - 40° . Since the value of $(P_T - P_s)$ and $(P_m - P_s)$ represent the respective tangential and meridional velocities, thus it indicates that the velocity of the leakage flow in impeller 30° - 20° is higher than that of impeller 30° - 40° . At last this condition can be suspected as the causal factor for the lower performance of impeller 30° - 20° , which has long passage.

The reason for the occurrence of higher leakage flow in the impeller with long passage, may be because of the low ability of the impeller to flow the fluid due to its long passage. Since the fluid can not flowed well, some of them tends to migrate to the suction side of the adjacent blade through the tip clearance and forms the leakage flow. Thus the leakage flow of impeller with long passage becomes larger than that of the impeller with medium length passage.

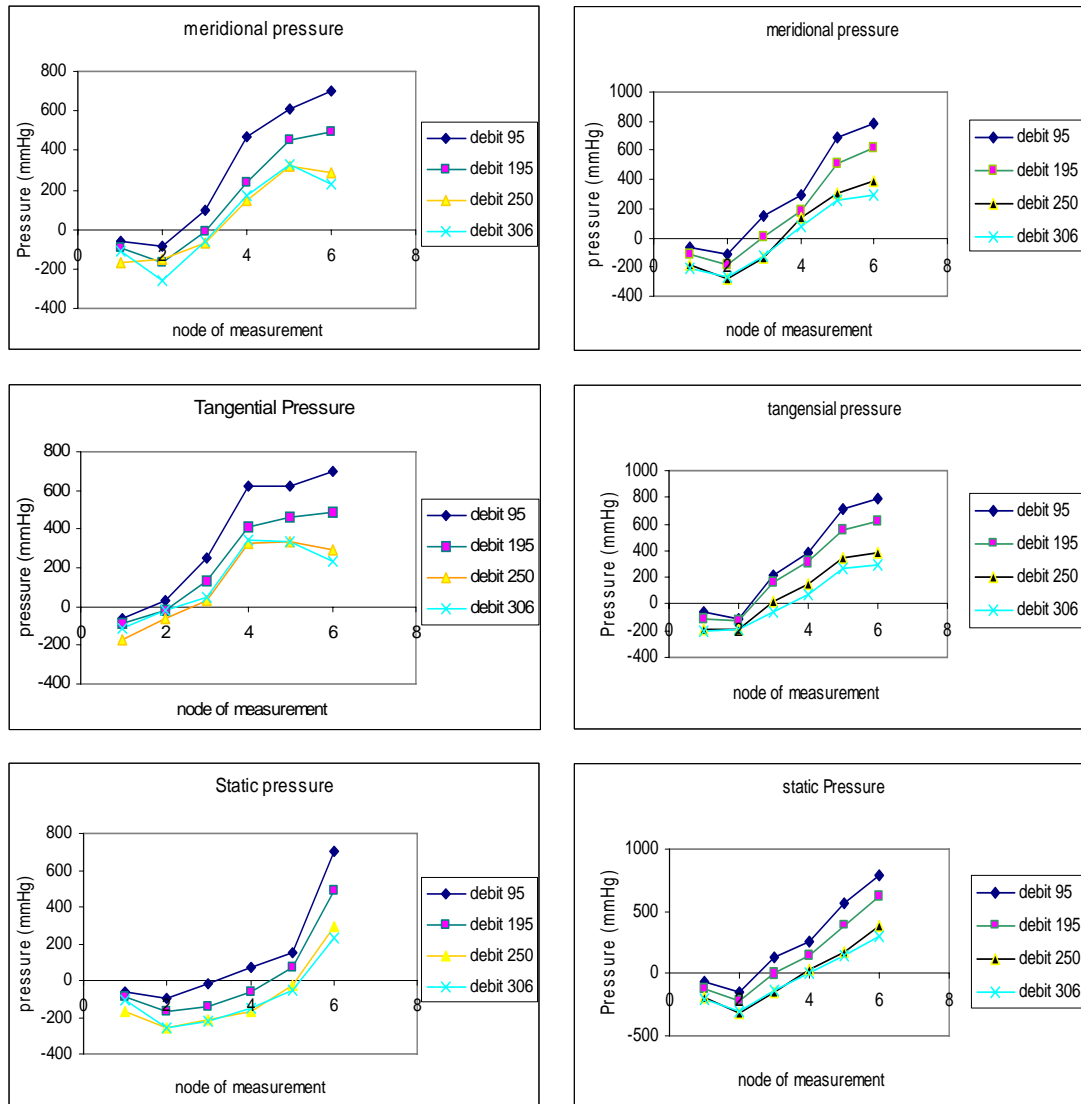


Figure 4-8. Effect of blade shape on the characteristic of pressure along the shroud
impeller 30-20 (left) and impeller 30-40 (right), both were at $c/b = 4.2/17$

CONCLUSIONS

1. The main flow in the passage is highly affected by the secondary flow and the vortex generation. The intensities of the secondary flow, includes vortices and separation are affected by blade curvature. The occurrence of such secondary flow will at last reduce the performance of the pump.
2. Impeller having large angle of divergence suffers larger suction side leg of horseshoe vortex which at last form its self as the passage vortex. This vortex flows from the suction side to the pressure side and causes deflection to the path of the main flow. The larger passage area will also give the possibility to the fluid to flow with reversion, that is the fluid tends to flow back.
3. Impeller with long passage suffers larger of friction loss due to its larger of contacting area between the fluid and passage surface. In this impeller the dimension and intensity of the suction side leg of the horseshoe vortex is slightly smaller than the pressure side leg of the horseshoe. At the outermost region the both vortex combine and at last together with the friction losses will deteriorate the performance of the pump.

4. The pressure along the shroud increases as the distance of the measurement node from the inlet is increased. Impeller with long passage causes lower of tangential, meridional and static pressures along the shroud than those of the impeller with shorter passage. Although the pressures is lower, but the value of $(P_T - P_s)$ and $(P_m - P_s)$ of long passage impeller are greater than those parameters of the shorter impeller. Indirectly, it indicates that the leakage capacity of long passage impeller is greater than that of shorter passage impeller.

ACKNOWLEDGMENT

The authors would wish to thank Masruri and Nia Kurniasih for their helpful assistance.

REFERENCES

- Austin, H Church, 1986, Pompa dan Blower Sentrifugal, Erlangga, Jakarta
- Balje, O. E., 1981, Turbomachines, A Guide to Design, Selection and Theory, John Wiley and Sons, NY.
- Chang, P. K., 1976, Control of Flow Separation, Hemisphere Publ. Co., Washington
- Copenhaver, W., 1996, "The Effect of Tip Clearance on a Swept Transonic Compressor Rotor", Journal of Turbo Machinery Vol 118, pp 230-239
- Hah, C. dan Krain, H., 1990, "Secondary Flows and Vortex Motion in a High-Efficiency Backswept Impeller at Design and Off-Design Condition", Journal of Turbo Machinery Vol 112, pp 7-13
- Hinze, J. O., 1959, Turbulence, Mc.Graw-Hill, NY
- Ishida, M., Ueki, H. dan Senoo, Y., "Effect of Blade Tip Configuration on Tip Clearance Loss of a Centrifugal Impeller", Transaction of the ASME Vol 112 pp. 14-18
- Ishida, M., Ueki, H. dan Senoo, Y., "Secondary Flow Due to the Tip Clearance at the Exit of Centrifugal Impeller", Transaction of the ASME Vol 112 pp. 19-24
- Lakshminarayana, 1996, Fluid Dynamics and Heat Transfer of Turbomachinery, John Wiley & Sons, NY
- Lazarkiewicz, 1965. Impeller pumps, Pergamon Press, London
- Murakami, M., Kikuyama, M., Asakura, E., 1980, "Velocity and Pressure Distributions in the Impeller Passages of Centrifugal Pumps", Transaction of the ASME Vol 102, pp 420-426
- Schlichting, H., 1979, Boundary Layer Theory, Mc.Graw-Hill, NY
- Sjolander, 1995, "Measurements of the Flow in an Idealized Turbine Tip Gap", Journal of Turbo Machinery Vol 117, pp 578-585
- Soeadgihardo Siswantoro, 2000, "Pengaruh Modifikasi Bentuk Impeler Pada Aliran dan Unjuk Kerja Pompa Sentrifugal.", Tesis, Universitas Gadjah Mada
- Stepanoff, 1957, Centrifugal and Axial, John Wiley & Sons, NY
- Van Dyke,, 1982, An Album Of Fluid Motion, Parabolic Press, Stanford CA